Chinese Chemical Letters 33 (2022) 747–750

Contents lists available at ScienceDirect

Chinese Chemical Letters

journal homepage: www.elsevier.com/locate/cclet

Allosteric conformational changes of G proteins upon its interaction with membrane and GPCR

Longmei Li[a,b], Jin Zhang[a], Wenjing Sun[a], Weimin Gong[a], Changlin Tian[a], Pan Shi[a,*], Chaowei Shi[a,*]

[a] Hefei National Laboratory of Physical Science at Microscale and School of Life Sciences, University of Science and Technology of China, Hefei 230027, China
[b] Department of Chemical Physics at School of Chemistry and Materials Sciences, University of Science and Technology of China, Hefei 230027, China

ARTICLE INFO

Article history:
Received 2 April 2021
Revised 13 July 2021
Accepted 15 July 2021
Available online 21 July 2021

Keywords:
^{19}F solution NMR
G protein-coupled receptors
Conformational dynamics
G protein

ABSTRACT

Current resolved structures of GPCRs and G protein complexes provided important insights into G protein activation. However, the binding or dissociation of GPCRs with G protein is instantaneous and highly dynamic in the intracellular environment. The conformational dynamic of G protein still needs to be addressed. In this study, we applied ^{19}F solution NMR spectroscopy to monitor the conformational changes of G protein upon interact with detergent mimicking membrane and receptor. Our results show that there are two states equilibria in the G_α in apo states. The interaction of G_α with detergents will accelerate this conformational transformation and induce a state that tends to bind to GPCRs. Finally, the G_α proteins presented a fully activation state when they coupled to GPCRs.

© 2021 Published by Elsevier B.V. on behalf of Chinese Chemical Society and Institute of Materia Medica, Chinese Academy of Medical Sciences.

G protein-coupled receptors (GPCRs) perceive many extracellular signals and transduce them to heterotrimeric G proteins, which in turn initiate a multitude of signaling cascades that alter cellular function. The β_2 adrenergic receptor (β_2AR) is a prototypical class A GPCRs [1], which preferentially couples to the stimulatory G protein ($G_{\alpha s}$) compared to inhibitory G protein ($G_{\alpha i}$) [2–4]. The first crystal structure of the quaternary complex composed of agonist-activated monomeric β_2AR and heterotrimeric G protein [5] opened a new avenue in the study of the interaction between GPCRs and G proteins. These high-resolution complex structures would provide structure basis for the downstream signaling-selective GPCR-targeting drug development. However, the static crystal structure and cryo-EM structure could not provide sufficient information about the dynamic process of G protein coupling to GPCRs. Furthermore, the $G_{\alpha i}$ coupling is much less efficient than $G_{\alpha s}$ coupling in most cytological and biochemical analysis making the complex of β_2AR-G_i is less stable than β_2AR-G_s [6]. Therefore, the current research on the mechanism of the interactions between β_2AR and $G_{\alpha i}$ is limited [7].

G proteins transduce signals from GPCRs to a variety of effector proteins, which might be localized to membrane microdomains with different lipid composition [8]. Membrane association and binding have been proved to play a crucial role in G protein function [9–11]. Direct membrane contact of the photoreceptor G protein heterotrimer has been observed by low resolution (~30 Å) electron crystallography [12]. Although there have been numerous studies of G protein-membrane interactions using mutagenesis, biochemical and functional approaches [13,14], the molecular basis underlying the interaction of the distinct G proteins subunits with the plasma membrane are still not fully understood [15]. This may in part be due to the fact that the structural heterogeneity of lipid-GPCRs ternary complex hindered the high-resolution structure determination by Cryo-EM or X-ray crystallography [16–18].

Nuclear magnetic resonance (NMR) spectroscopy in solution is one of the key approaches to explore dynamic features, which can be accessed at physiological temperature and with minimal modification of proteins [19–21]. ^{13}C-methylated lysine, $^{13}CH_3$-labelled methionine and cysteine-based modification approach such as 2,2,2-trifluoroethanethiol (TET) or 3-bromo-1,1,1-trifluoroacetone (BTFA) labelling have been extensively performed for conformational dynamics study of GPCRs [22–24]. Previous spectroscopic strategies have shown that β_2AR adopts multiple conformational states activated by agonist in the presence or absence of G protein [25]. However, the dynamic conformational change of G protein coupling to GPCRs is remained elusive.

Herein, we utilize ^{19}F NMR spectroscopy to monitor the conformational change of the G_α proteins coupling to the β_2AR. The ^{19}F atoms are introduced by site-specific incorporation method with high specificity, efficiency and fidelity [26]. Compared with other methods for the fluorine introduction [27–30], site-specific incor-

* Corresponding authors.
E-mail addresses: shipan@ustc.edu.cn (P. Shi), scwei@ustc.edu.cn (C. Shi).

https://doi.org/10.1016/j.cclet.2021.07.042
1001-8417/© 2021 Published by Elsevier B.V. on behalf of Chinese Chemical Society and Institute of Materia Medica, Chinese Academy of Medical Sciences.

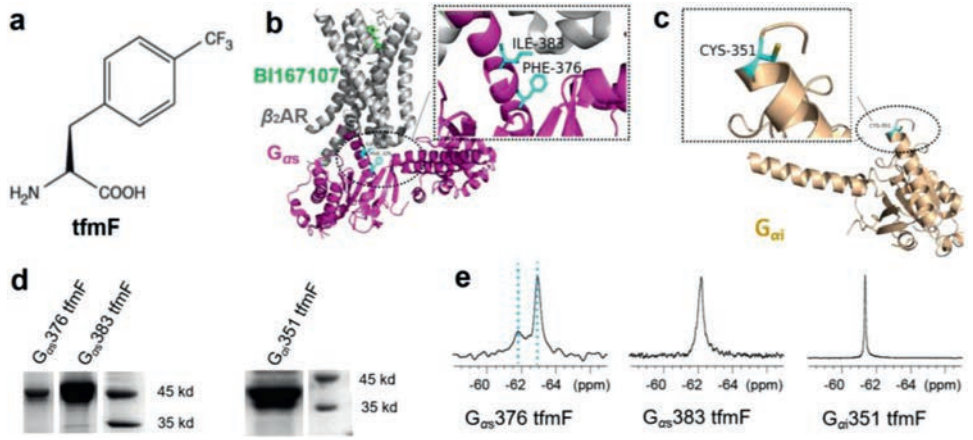

Fig. 1. Site-specifically incorporates tfmF into G_α proteins in response to a UAG stop codon in *E. coli*. (a) The chemical structure of L-4-trifluoromethylphenylanine (tfmF). (b) Ribbon representation of $G_{\alpha s}$ subunit in the β_2AR-$G_{\alpha s}$ complex (PDB accession number 3SN6). The ^{19}F probe tfmF was incorporated at residue F376 and I383 located at the interface of β_2AR and $G_{\alpha s}$ labelled in cyan. (c) Ribbon representation of $G_{\alpha i}$ subunit (PDB accession number 6DDE). The ^{19}F probe tfmF was incorporated at residue C351 labelled in cyan. (d) SDS-PAGE analysis of tfmF incorporation into $G_{\alpha s}$ (47 kDa, left) and $G_{\alpha i}$ (41 kDa, right). (e) ^{19}F NMR spectra of conformational equilibria for $G_{\alpha s}$376 tfmF, $G_{\alpha s}$383 tfmF and $G_{\alpha i}$351 tfmF. The observation of two uncoupled conformational equilibria shows that there are two distinct states for apo-form G_α protein. The two states S1 and S2 are indicated by two cyan dash lines.

poration of a ^{19}F labelled amino acids into proteins is a powerful tool for monitoring protein conformational changes, protein processing and protein stability studies *in vivo* and *in vitro* [19,31]. Our data show that the apo-form of G_α protein adopts two conformations. Further structural changes were observed when G_α protein interacted with detergent mimicking cell membrane, which confirmed that interaction with the cell membrane is pivotal for G protein activation. The conformation of both $G_{\alpha s}$ and $G_{\alpha i}$ proteins were further stabilized by coupling to activated β_2AR. Our studies provided insights into the dynamic process of GPCR-G protein signaling pathway.

To obtain ^{19}F labelled target proteins, we used two plasmids in the system: One plasmid expressing the *Methanococcus Jannaschii* tyrosyl amber suppressor tRNA (MjtRNA-Tyr_{CUA})/tyrosyl-tRNA synthetase (MjTyrRS) pair, and the other plasmid containing a TAG mutant of the G protein gene (Fig. S1 in Supporting information) [32]. *E. coli* cells carrying both plasmids are grown in the presence of L-4-trifluoromethyl-phenylalanine (tfmF) (Fig. 1a) to produce the ^{19}F-labelled G_α protein. Due to the rapid rotation of the CF_3 group, the sensitivity of NMR signals can be improved by tfmF labelling.

We individually introduced unnatural amino acid tfmF to the receptor coupling interface of the $G_{\alpha s}$ and $G_{\alpha i}$ that can be used as ^{19}F NMR reporters to monitor structural changes in response to β_2AR. One-dimensional NMR spectra were collected with the proton coil tuned to the ^{19}F frequency for 1-3 h to further confirm that the tfmF was successfully incorporated into target proteins. Finally, the ^{19}F-labelled proteins with high labelling efficiency and friendly thermal stability were selected for the following NMR experiment, such as $G_{\alpha s}$376 tfmF, $G_{\alpha s}$383 tfmF and $G_{\alpha i}$351 tfmF (Figs. 1b-d). All these residues located in the C- terminal of α5 helix, which is a key determinant of GPCR-G protein coupling selectivity [33]. Previous fluorescence lifetime based FRET studies have revealed that both $G_{\alpha s}$ and $G_{\alpha i}$ presented two distinct conformations in the apo-state [34]. Consistent with previous studies, our results show that there are two conformations (hereinafter called states S1 and S2) for each tfmF incorporation site (Fig. 1e). In the apo-form, we observed two obvious peaks for $G_{\alpha s}$376 tfmF, suggesting the existence of conformational heterogeneity in this location with slow exchange between two conformational states on slow time scale ($k << 1.5\ ms^{-1}$) at room temperature. Similar to the structural heterogeneity in ^{19}F NMR spectra of $G_{\alpha s}$376 tfmF, $G_{\alpha s}$383 tfmF show a broad line shape, derived from the overlap of two signals. The resulting ^{19}F NMR spectra identify two states of $G_{\alpha s}$ protein that likely correspond to the free-binding states S1 and S2. Compared to the 1D ^{19}F NMR spectra of $G_{\alpha s}$ site-specifically incorporation proteins, there is only one ^{19}F peak in the 1D NMR spectra of $G_{\alpha i}$351 tfmF. The difference in the ^{19}F NMR spectra of $G_{\alpha s}$ and $G_{\alpha i}$ proteins is probably due to the $G_{\alpha i}$351 located at the C-tail of α5 helix in $G_{\alpha i}$ containing a total of 354 amino acids, which is highly flexible and the two free-binding states S1/S2 are in fast exchange timescale resulting only one sharp peak on the NMR spectrum.

Recently, nanodisc has been widely used for structural and functional studies of membrane proteins [35]. Membrane scaffold protein MSP1D1 and the lipid mixture of 1-palmitoyl-2-oleoyl-sn-glycero-3-phosphocholine (POPC) and 1-palmitoyl-2-oleoyl-sn-glycero-3-phospho-(1′-rac-glycerol) (POPG) were used to assemble the nanodisc with the suitable diameter for titration analysis (Fig. S2 in Supporting information). May due to the invisibility of giant size G_α-nanodisc complex, we could mainly observed the gradually peak intensity decreases of G_α protein titrated with nanodiscs from the ^{19}F NMR spectroscopy (Fig. S3 in Supporting information). Fortunately, we observed a new broad peak on the $G_{\alpha s}$376 tfmF spectrum titrated with nanodisc, indicating the new G_α-nanodisc complex state (Fig. S3a in Supporting information). In order to determine the dynamic process of G_α protein interacting with plasma membrane, we use micelle composed of small molecule detergents mimicking membrane to monitoring the conformational changes of different G_α proteins compared of their apo state. The mixed micelles of *n*-dodecyl-β-D-maltoside (DDM) and cholesteryl hemisuccinate (CHS), with DDM/CHS (2:1), was gradually titrated into G_α protein. The structural changes that occurred upon the addition of detergent to the G_α protein were performed using ^{19}F NMR. Interestingly, the ^{19}F NMR spectrum of G_α protein changes accompany with the detergent concentration increases. Starting with the two weakly peaks on the spectrum of $G_{\alpha s}$376 tfmF, addition of the detergent resulted in the appearance of a broad line shape signal peak, indicated that the rate of chemical exchange between S1 and S2 has increased induced by detergent monomers (Fig. 2a). Subsequent addition of an excess of the detergent made the peak shape of the resonance sharp and the signal stronger. Therefore, it can be reasonably deduced based on the peak shape and intensity, there covered another new state of $G_{\alpha s}$376 tfmF apart from S1-S2, which we referred as state S3. Since the new broad peak of G_α-micelle

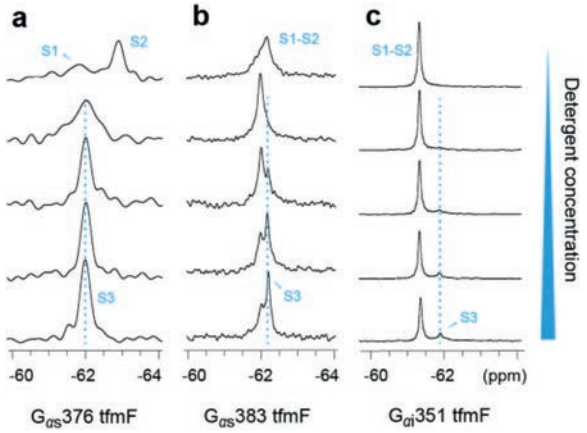

Fig. 2. ^{19}F NMR spectra of the $G_{\alpha s}$ or $G_{\alpha i}$ in the apo-form or with increasing amount of detergent: Detergent titration of (a) $G_{\alpha s}$376 tfmF, (b) $G_{\alpha s}$383 tfmF, and (c) $G_{\alpha i}$351 tfmF. The concentration of detergent increases from top to bottom (0, 0.04%, 0.08%, 0.12%, 0.2%). The transition states S3 was indicated by cyan dash lines.

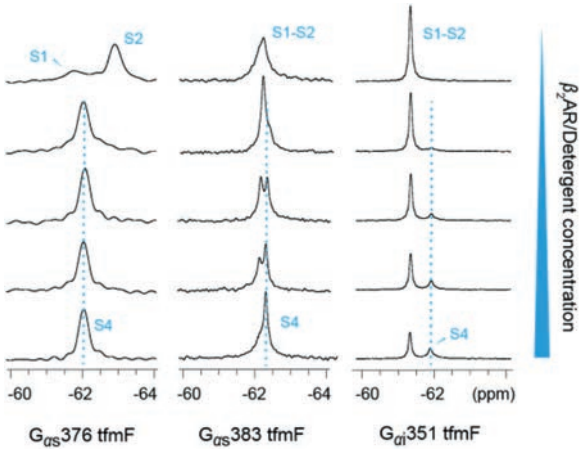

Fig. 3. ^{19}F NMR spectra of the $G_{\alpha s}$ and $G_{\alpha i}$ in the apo-form or with increasing amount of β_2AR/detergent. Five 1D ^{19}F spectra for each mutant were recorded with G_α:β_2AR ratios of 1:0, 1:0.25, 1:0.5, 1:0.75 and 1:1.

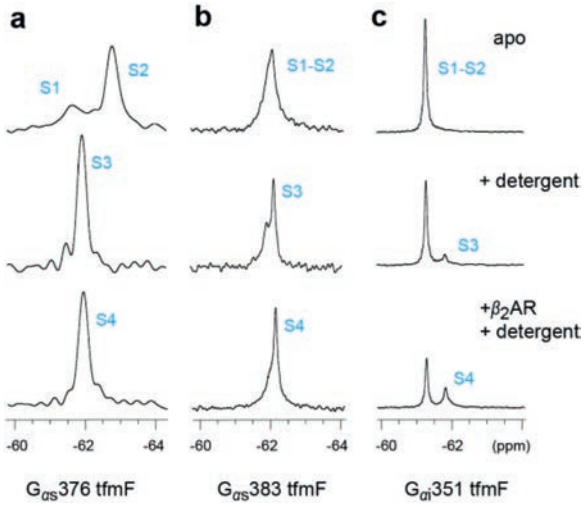

Fig. 4. ^{19}F NMR spectra of the $G_{\alpha s}$ and $G_{\alpha i}$ in the apo-form or in the presence of detergent, β_2AR/detergent respectively: (a) $G_{\alpha s}$376 tfmF, (b) $G_{\alpha s}$383 tfmF and (c) $G_{\alpha i}$351 tfmF. Compared with adding detergent alone (the second row), the widths and intensity of the NMR peaks for G_α proteins were slightly changed in the presence of the β_2AR (the third row).

complex state shows the same chemical shift with G_α-nanodisc complex, we consider that the mixed micelles could mimic the native plasma membrane in our case (Fig. S3b in Supporting information). Similarly, as detergent is gradually added to the $G_{\alpha s}$383 tfmF, the broad line shape getting sharper at low detergent concentration, indicating faster chemical exchange of state S1 and S2. The binding of detergent micelles promotes the generation of equilibrium between S1 and S2, driving the $G_{\alpha s}$ from S1-S2 towards S3 (Fig. 2b). In addition, observation of the ^{19}F NMR signals originating from $G_{\alpha i}$ provided similar results to those obtained from observation of $G_{\alpha s}$. In contrast to $G_{\alpha s}$376 tfmF and $G_{\alpha s}$383 tfmF, addition of the detergent micelles resulted in a pronounced shift towards S3 for $G_{\alpha i}$351 tfmF, making position of the NMR peaks is clearly separated from the S1-S2 (Fig. 2c). Collectively, detergent will accelerate the rate of equilibrium between S1-S2 and induce a new state S3, which is associated with the membrane interaction. This state probably represents the transition state before the G protein and receptor interaction.

To characterize the dynamic properties of different G proteins coupling to GPCR, we acquired ^{19}F NMR spectra of G_α proteins bound to β_2AR in the presence of the BI167107, an ultra-high-affinity full agonist that increase basal $G_{\alpha s}$ coupling activity [36]. Due to the activation of the β_2AR results in TM6 movement that lead to a receptor-binding site for intracellular effector or regulatory proteins, a given concentration of agonist is added throughout the experiment [37]. We observed spectral changes in G_α protein upon detergent binding, and further changes were observed following β_2AR coupling (Figs. 3 and 4). No significant chemical shift changes of $G_{\alpha s}$376 tfmF was observed upon β_2AR binding. However, the interaction with β_2AR slow down the global tumbling of $G_{\alpha s}$376 tfmF leading to a slightly broad line shape of the NMR peaks (Fig. 4a). This shows that $G_{\alpha s}$376 tfmF has produced a receptor-binding conformation, named state S4. Moreover, the G_α protein and β_2AR were indeed coupled into a complex which was verified through size exclusion chromatography (SEC) (Fig. S4 in Supporting information).

In the presence of the β_2AR, the signal peaks representing S1-S2 of $G_{\alpha s}$383 tfmF disappear almost completely. The newly upfield peak almost completely replaces the downfield peak, illustrated the population of states shifted towards the binding state S4 at the expense of S1-S2 and S3. Similar to $G_{\alpha s}$383 tfmF, upon coupling to β_2AR we see the $G_{\alpha i}$351 shifted the S1-S2 equilibrium towards the S4 state by an increment in intensity comparing with the $G_{\alpha i}$-detergent binding state (Fig. 4c). However, same amount of β_2AR and detergent can only induce a small fraction of β_2AR-$G_{\alpha i}$ complex (~36% based on the integrated peak area). This may be due to the dynamic nature of the $G_{\alpha i}$351 tfmF that a small fraction of $G_{\alpha i}$351 existing in a state is capable of coupling with the β_2AR, which confirmed the weak coupling specificity of β_2AR-$G_{\alpha i}$ complex. In summary, except for the widths and intensity of the NMR peaks, chemical shift of G_α protein remain practically unchanged after coupling to the β_2AR compared to detergent binding state and confirmed that there may be a shallow energy barrier between S3 and S4, allowing rapid chemical exchange of the two state populations. In this study, the relatively weak interaction between $G_{\alpha i}$351 and β_2AR was detected using ^{19}F NMR spectroscopy (Fig. 4c). Compared with $G_{\alpha s}$376 and $G_{\alpha s}$383, less population of $G_{\alpha i}$351 could form complex S4 states with β_2AR. These differences in one-dimensional NMR spectra consistent with the result of a previous study that β_2AR can interact with both $G_{\alpha i}$ and $G_{\alpha s}$ and it may have a preference over coupling $G_{\alpha s}$.

As noted above, the tfmF was site-specific incorporated into G_α proteins with high fidelity and used to monitor G protein-membrane interactions and G protein-receptor binding conformational changes. In 1D NMR, each peak defines a given conformation

or state. Our data suggests that G_α proteins adopt allosteric conformational changes upon interacting with membrane and coupling with GPCRs (Fig. S5 in Supporting information). One-dimensional ^{19}F NMR studies provide evidence for conformational heterogeneity as we observe more than one peak for F376, I383 in apo $G_{\alpha s}$ and C351 in apo $G_{\alpha i}$. Previous study showed that the G_α protein was anchored on the cell membrane through palmitoylated post-translational modification. Based on our data, the C-terminal α5 helix also involve in the G_α-membrane interaction. The ^{19}F NMR spectra of $G_{\alpha s}$ and $G_{\alpha i}$ in the presence of detergent may represented the membrane binding state of $G_{\alpha s}$ and $G_{\alpha i}$, which is ready to coupling to GPCR. The membrane interactions with G_α simulated by nanodisc or micelle both induce a transition from the equilibrium state of the two free conformations to the membrane-binding state, which may be similar to the transition state before the G protein coupling to the receptor. Combine the results of G_α-β_2AR coupling, we suspect that the interaction with membrane may be indispensable for the activation of different G_α proteins. These data provide evidence for the importance of G protein and membrane interaction for GPCR coupling. Additionally, we captured the protein conformational changes and differences in the interactions between β_2AR -$G_{\alpha i}$ and the β_2AR-$G_{\alpha s}$ complex by monitoring of the ^{19}F NMR chemical shifts. The ^{19}F NMR may thus prove to be a convenient and effective tool for the studies of dynamic process of GPCR-G protein signaling pathway .

Declaration of competing interest

The authors declare no conflict of interest.

Acknowledgments

This work was supported by the National Key Research and Development Project of China (Nos. 2019YFA0904100 and 2017YFA0505400), the National Natural Science Foundation of China (Nos. 22077117 and 31971152) and the USTC Research Funds of the Double First-Class Initiative.

Supplementary materials

Supplementary material associated with this article can be found, in the online version, at doi:10.1016/j.cclet.2021.07.042.

References

[1] E.A. Wold, J. Chen, K.A. Cunningham, J. Zhou, J. Med. Chem. 62 (2019) 88–127.
[2] M.G. Guereschi, L.P. Araujo, J.T. Maricato, et al., Eur. J. Immunol. 43 (2013) 1001–1012.
[3] Y. Daaka, L.M. Luttrell, R.J. Lefkowitz, Nature 390 (1997) 88–91.
[4] B.R. Erdogan, M.C. Michel, E. Arioglu-Inan, Cell 9 (2020) 2548–2577.
[5] S.G. Rasmussen, B.T. DeVree, Y. Zou, et al., Nature 477 (2011) 549–555.
[6] L.M. Wingler, M.A. Skiba, C. McMahon, et al., Science 367 (2020) 888–892.
[7] M.J. Strohman, S. Maeda, D. Hilger, et al., Nat. Commun. 10 (2019) 2234.
[8] R. Álvarez, D.J. López, J. Casas, et al., Biochim. Biophys. Acta 1851 (2015) 1511–1520.
[9] M. Crouthamel, M.M. Thiyagarajan, D.S. Evanko, P.B. Wedegaertner, Cell Signal. 20 (2008) 1900–1910.
[10] X. Ma, Y. Hu, H. Batebi, et al., Proc. Natl. Acad. Sci. U. S. A. 117 (2020) 23096–23105.
[11] W. Hu, H. Wang, Y. Hou, Y. Hao, D. Liu, FEBS Lett. 593 (2019) 1113–1121.
[12] Z. Zhang, T.J. Melia, F. He, C. Yuan, A. McGough, et al., J. Biol. Chem. 279 (2004) 33937–33945.
[13] T. Didenko, J.J. Liu, R. Horst, R.C. Stevens, K. Wuthrich, Curr. Opin. Struct. Biol. 23 (2013) 740–747.
[14] X. Wang, A. McFarland, J.J. Madsen, E. Aalo, L. Ye, Trends. Pharmacol. Sci. 42 (2021) 19–30.
[15] E.N. Marsh, Y. Suzuki, ACS Chem. Biol. 9 (2014) 1242–1250.
[16] X. Ma, Y. Hu, H. Batebi, et al., Proc. Natl. Acad. Sci. U. S. A. 117 (2020) 23096–23105.
[17] J.L. Kitevski-LeBlanc, R.S. Prosser, Prog. Nucl. Magn. Reson. Spectrosc. 62 (2012) 1–33.
[18] R. Horst, J.J. Liu, R.C. Stevens, K. Wuthrich, Angew. Chem. Int. Ed. 52 (2013) 10762–10765.
[19] J.C. Jackson, J.T. Hammill, R.A. Mehl, J. Am. Chem. Soc. 129 (2007) 1160–1166.
[20] T.H. Kim, K.Y. Chung, A. Manglik, et al., J. Am. Chem. Soc. 135 (2013) 9465–9474.
[21] L. Li, S.H. Chang, J.F. Xiang, et al., Chin. Chem. Lett. 23 (2012) 89–92.
[22] A. Manglik, T.H. Kim, M. Masureel, et al., Cell 161 (2015) 1101–1111.
[23] M.P. Bokoch, Y. Zou, S.G.F. Rasmussen, et al., Nature 463 (2010) 108–112.
[24] Y. Kofuku, T. Ueda, J. Okude, et al., Nat. Commun. 3 (2012) 1045.
[25] J.J. Liu, R. Horst, V. Katritch, R.C. Stevens, K. Wüthrich, Science 335 (2012) 1106–1110.
[26] L. Wang, P.G. Schultz, Chem. Commun. (2002) 1–11.
[27] K.V. Loscha, A.J. Herlt, R. Qi, et al., Angew. Chem. Int. Ed. 51 (2012) 2243–2246.
[28] M. Zhang, M. Wen, Y. Xiong, L. Zhang, C. Tian, Chin. Chem. Lett. 29 (2018) 1509–1512.
[29] S. Wang, Y. Zhang, L. Zhang, M. Zhang, C. Tian, Chin. Chem. Lett. 29 (2018) 1513–1516.
[30] P. Zhou, P. Lv, L. Yu, et al., Chin. Chem. Lett. 30 (2019) 1067–1070.
[31] J. Suarez, A.M. Haapalainen, S.M. Cahill, et al., Chem. Biol. 20 (2013) 212–222.
[32] J.T. Hammill, S. Miyake-Stoner, J.L. Hazen, J.C. Jackson, R.A. Mehl, Nat. Protoc. 2 (2007) 2601–2607.
[33] T. Flock, A.S. Hauser, N. Lund, et al., Nature 545 (2017) 317–322.
[34] P. Shi, Y. Zhang, P. Lv, et al., Chem. Commun. 56 (2020) 6941–6944.
[35] K. Mio, C. Sato, Biophys. Rev. 10 (2018) 307–316.
[36] I.L.J.G. James, A.R. Dalton, BMC Bioinformatics 16 (2015) 124.
[37] M.A. Hanson, V. Cherezov, M.T. Griffith, et al., Structure 16 (2008) 897–905.